A possible new molecular mechanism of thundercloud electrification

Pavel Jungwirth[(a)]*, Daniel Rosenfeld[(b)], Victoria Buch[(c)]

(a) J. Heyrovský Institute of Physical Chemistry, Academy of Sciences of the Czech Republic and Center for Complex Molecular Systems and Biomolecules, Dolejškova 3, 18223 Prague 8, Czech Republic, (b) Institute of Earth Sciences, The Hebrew University of Jerusalem, Jerusalem 91904, Israel, (c) Department of Physical Chemistry and Fritz Haber Center for Molecular Dynamics, The Hebrew University of Jerusalem, Jerusalem 91904, Israel

Abstract

Thunderclouds are electrified when charge is transferred between small and large ice particles colliding in a cloud that contains strong updrafts. The small ice particles rise with one type of charge and the large ice particles fall and carry with them downward the other type of charge, which is most often negative, so that normally lightning lowers negative charge from cloud to the ground. While the mechanism of ice charging is well established, the nature of the charge transfer between the colliding ice particles is not very well understood on the atomic level, and no present theory can explain fully the charge transfer, or even the sign of the charging. Here we propose a new charge separation mechanism that is based on molecular simulations of the collisions, keeping track of the individual charges as they move in the form of salt ions from one ice particle to another. Under normal conditions, when sulfates dominate as cloud condensation nuclei, this ionic mechanism is consistent with the prevailing negative lightning in thunderclouds. Moreover, with dearth of sulfate anions, the present mechanism predicts a shift towards positive charging. This fits well to a large range of observations of enhanced positive lightning, connected with smoke rich in chlorides and nitrates, that could not be explained satisfactorily previously.

1. Introduction

The various suggestions to the causes of charge transfer pertain to differences in the surface properties of the colliding falling and rising ice particles. The rising particles are pristine ice crystals that form on ice nuclei or frozen drops, and grow by deposition of water vapor. The typical form of falling ice precipitation particles in thunderclouds is the graupel, which forms when supercooled cloud droplets aggregate on ice crystals or frozen raindrops and freeze upon impact before having time to lose their spherical shape. Hail forms at relatively warm temperatures or in clouds with very high supercooled water content, when the cloud drops spread on the surface before freezing, forming a wet surface over a glazed ice hailstone. Laboratory experiments show that charge transfer occurs in collisions between ice crystals and graupels, but not with wet hailstones (Berdeklis and List, 2001).

Laboratory studies of charge transfer during collision between graupel and ice crystals at various conditions, using distilled water, have established empirically that in water saturation regime graupel is charged negatively at T<-10ºC, with peak charging rate at around -16ºC (Berdeklis and List, 2001; Takahashi, 1978). The charging rate decreases at colder temperatures, and becomes relatively small at T<-20ºC. Charging is, however, positive at temperatures above -10ºC. The charging rate and sign depend strongly on the relative humidity (RH), which determines the diffusional growth rate of the ice surfaces and the structure of the ice crystals. Greater RH leads to a larger magnitude of negative charge transfer during a collision of graupel and ice crystal (Berdeklis and List, 2001), peaking at –25 fC per single collision at water saturation saturation (which is the prevailing condition in the updrafts of thunderclouds), T=-16ºC, and collision velocity of 5 ms^{-1}. Greater RH also leads to a shift to higher temperatures of the cross over from positive to negative charging. At vapor saturation above ice negative charging vanishes at -16ºC or even crosses over to positive charging. The effective cloud water content, or the rate of

riming which determines the surface temperature excess of the graupel, works the same way as relative humidity, with positive charging at all tested temperatures down to -25ºC and for effective liquid water content < ~ 0.2 gm^{-3}.

Positive charging was obtained in laboratory experiments (Takahashi and Miyawaki, 2002) also on the other extreme: very large amounts of highly supercooled cloud water content (> ~2.5 gm^{-3}) induce positive charging even at T< -20ºC. This is consistent with the reports of polarity reversal for severe thunderstorms with wide and intense updrafts, leading to elevation of the charging zone to regions where such conditions prevail (Lang and Rutledge, 2002). The formation of precipitation particles in these strong and wide updrafts is delayed to greater heights, so that liquid cloud water accumulates to very large values. According to laboratory experiments, the changeover to positive charging occurs with high supercooled cloud liquid water content (SLWC) at increasingly colder temperatures for greater SLWC, probably due to the increasingly intense latent heat release and warming on the surface of the graupel for greater SLWC. Laboratory experiments (Williams et al., 1991), when combined with the laboratory charging experiments of Takahashi and Miyawaki (2002) showed that warming of the graupel above about –10ºC induces its positive charging. A complex Fig. 1, adopted from Takahashi and Miyawaki (2002), summarizes all the above findings in a graphical way, showing the regions of negative or positive graupel charging as a function of temperature and the effective cloud water content.

Baker et al. (1987) proposed the principle that upon collision of two ice particles, the particle growing faster from vapor charges positively and the other negatively. Dash et al. (2001) provided further theoretical support for this principle. They suggested that the faster growing ice surface also has a larger density of dislocations, and hence also more broken water molecules. The role of ionic and Bjerrum defect in charging was also emphasised in a most recent study by Nelson and

Baker (2003). While the OH^- ions are bound to the crystal grid, the positive ions are mobile in the interfacial quasi-liquid layer, and upon collision there is a net transfer from the faster to slower growing counterpart. A graupel surface that warms due to latent heat release would grow slower than the ice crystals and thus charge negatively. On the other hand, water vapor from warmed freezing drops on the graupel would be deposited on other parts of the same graupel (Baker et. al, 1987) and make them the faster growing ice surface, and hence charge positively. This theory does not provide an explanation for the observed change from positive to negative charging of a graupel at -10ºC under the condition of water saturation.

Sommer and Levin (2001) suggested, based on theoretical calculations and laboratory experiments, that molecules and ions can be transferred between two approaching surfaces of water drops or ice crystals with surface quasi-liquid layers, when the distance of separation is in the range of 10 nm. The molecules and ions are transferred from the particle with greater surface curvature (e.g., a tip of a crystal) to the flatter particle (e.g., a frozen cloud drop on the graupel surface) when they approach each other just before the collision. The charge can remain separated, provided the contact during the collision is shorter than the charge neutralization time. Ions, after leaving one particle and before reaching the other, can be lost to intervening molecules in the vapor. Since OH^- ions have longer mean lifetimes than H_3O^+ ions, negative charge will be transferred preferentially from the quasi-liquid layer on the ice crystals to the graupel particles, leaving the ice crystals positively charged and the graupel negative, as reported for a majority of thunderclouds at around -15ºC.

None of the mechanisms proposed until now is capable of explaining the observed positive charging of the graupel at T>-10ºC, or at any temperature in low cloud liquid water content. The positive charging under these conditions is consistent with the propensity of positive cloud to ground lightning (i.e., lowering positive charge to the ground) in shallow thunderstorms over the cool sea surface (Orville and

Huffines, 2001), probably because of the shallow supercooled zone in these clouds, that occurs mostly below the charging reversal isotherm of about -10ºC.

Furthermore, the sign of charging apparently reverses under certain conditions that were not yet replicated in the laboratory experiments. Towards the end of the paper, we elaborate on observations linking the ionic composition of aerosols to the polarity of lightning. The soluble anions of smoke are mainly chloride and nitrate (Yamasoe et al., 2000), whereas the dominant anionic component of urban air pollution is sulfate. As we show below, the ions from smoke and urban sources have opposite charges at the surface of the solutions. This electrochemical difference in the polarity of the interfacial layer provided us with a clue that led us to the proposed ionic mechanism. The only previously suggested charging mechanism that involves salt ions is based on differential incorporation of ions into freezing ice (Workman and Reynolds, 1950). Laboratory experiments (Reynolds et al., 1957; Jayarante et al., 1983) showed that graupel formed in salty cloud water were charged negatively for NaCl and positively for $(NH_4)_2SO_4$, NH_4OH, and NH_4Cl, in agreement with the Workman effect (Workman and Reynolds, 1950). The apparent Workman effect vanished in salt concentrations smaller than 2×10^{-5} M. Our proposed mechanism is based on just the opposite - salt rejection from the freezing cloud droplet, which creates a nanoscopic solution layer on the surface of the frozen droplets. Furthermore, our effect would be manifested in the naturally occurring much smaller concentrations than required for the Workman effect, according to the laboratory experiments mentioned above.

2. Surfaces of ice particles

The suggested ionic mechanism relies on the fundamental difference in the composition of the ice crystal and the graupel. Ice crystals grow directly by deposition

of water vapor, forming a neat ice surface. The graupel surface is formed by frozen cloud droplets, which originally nucleated on pre-existing soluble aerosol particles - the cloud condensation nuclei (CCN). The surface of these frozen droplets is covered by a thin liquid layer containing soluble salts, primarily ammonium sulfate (which forms the most abundant CCN under normal conditions). The mechanism of the appearance of a concentrated solution at the surface during freezing of accreted water droplets can be viewed as a micro-analogue to salt rejection from ice during freezing of sea water above the eutectic point (Aagard and Carmack, 1989). In contrast to liquid H_2O, solubilities of ions and molecules in single crystal ice are known to be very low (Petrenko and Whitworth, 1999). For example, solubilities of HNO_3 and HCl at -15 ^oC were measured to be 0.3 and 5 ppm mole fractions, respectively (Thibert and Domine, 1997, 1998). There are no ice solubility data for $(NH_4)_2SO_4$ available to us, except for measurements of uptake up to 3 ppm, reported by Gross and Svec (1997). This number, however, most likely overestimates the solubility of ammonium sulfate, since most of the ions may be concentrated at grain boundaries (Gross and Svec, 1997; Mulvaney at al., 1988).

Thus, due to salt rejection upon freezing, the original liquid droplet, which is formed by a very dilute salt solution, becomes a piece of almost neat ice covered by a very thin layer of a rather concentrated salt solution. For temperatures between –10 and –15 ^oC, CCN in the size range of 0.1 – 0.5 μm, and a typical droplet with a diameter of 10 μm, which has grown on such an activated CCN, the thickness of the salt solution layer on the surface of the frozen droplet reaches 0.1 – 10 nm, with ammonium sulfate concentration of 2 - 4 M (17 - 34 wt%) (Clegg et al., 1998; Xu et al., 1998). However, one should take into account also the existence of the quasi-liquid layer that forms on neat ice surfaces. At these temperatures the thickness of this quasi-liquid layer reaches one to several nanometers (Furukawa and Nada, 1997), i.e., the same order of magnitude as the thickness of the salt solution layer. Due to a possible combined effect of these two layers the above concentration of the surface

salt solution is probably somewhat smaller. In order to remain on the safe side we have, therefore, assumed in the simulations salt concentrations reduced roughly by a factor of two.

3. Simulation protocol

We have modelled the interfacial salt solution layer using molecular dynamics (MD) simulation in a slab arrangement (Wilson and Pohorille, 1991). In the MD simulations in the slab geometry we employed periodic boundary conditions extended in one dimension. The unit box of a size of 3 x 3 x 10 nm contained 864 water molecules, 36 ammonium cations, and 18 sulfate dianions, corresponding to salt concentration of 1.2 M. Simulations were performed for liquid slabs for temperatures between 275 and 300 K. No appreciable temperature effect on the structure of the solution was observed within this temperature range. Analogous simulations were also performed for aqueous slabs containing 1.2 M of KCl or KNO_3.

We modelled the ice crystal-graupel encounter in two different ways. In the first simulation, starting from the slab of aqueous ammonium sulfate solution, we removed all solute ions from one half of the slab. In order to avoid penetration of the ions to the neat aqueous part we kept frozen a 0.3 nm thick layer of water molecules in the middle of the slab. After equilibrating the system at ambient temperature for 0.5 ns we reduced very fast (within several picoseconds) the extended box dimension from 10 to 3.4 nm and followed the subsequent dynamics for 1 ns. This shrinking effectively puts the two slab surfaces (one neat and the other containing solute ions) into close contact.

In addition, we also simulated an ice crystal-graupel collision employing finite size particles. Since simulations of collisions of micrometer size particles are

computationally unfeasible, we scaled down their size by three orders of magnitude. Consequently, the atmospheric graupel covered by a thin layer of ammonium sulfate solution was modelled as a liquid droplet. The two colliding particles were, therefore, an ice nanocrystal (containing 292 water molecules) and a nanodroplet formed by a 0.66 M ammonium sulfate solution (864 water molecules, 20ammonium cations, and 10 sulfate dianions).

In all molecular dynamics simulations a polarizable force field was employed. Namely, for water we used the SPC/POL potential (Caldwell et al., 1990), sulfate model was the same as in Jungwirth et al. (2003), and for ammonium we employed a non-polarizable potential from Boudon and Wipff (1991) adding a polarizability of 1.34 A^3 on the nitrogen atom. For potassium and nitrate we employed a non-polarizable potential from Straatsma and Berendsen (1988) and Signorini et al. (1990) augmented by polarizabilities of 0.85 A^3 on potassium and 1.3 A^3 on each of the nitrate oxygens. We parameterized all these polarizabilities using an ab initio quantum chemistry approach, described in detail in Jungwirth et al. (2003) and Jungwirth and Tobias (2002). A polarizable potential for chloride has been adopted from Dang (2002). Calculations have been performed using the molecular dynamics code Amber6 (Case et al., 1999) and quantum chemical program package Gaussian98 (Frisch et al., 1998).

The quality of the employed polarizable force field is sufficient to reproduce the occurence and polarity of an electric double layer close to the salt solution/air interface (Randles, 1957; Randles, 1977). In the case of singly charged ions, large and polarizable anions reside closer to the interface than small non-polarizable cations (Jungwirth and Tobias, 2002; Randles, 1957; Randles, 1977), which leads to a negative polarity of the ionic surface double layer. The results of the present simulations of 1.2 M solutions of KCl and KNO_3 are in a perfect agreement with the

measured negative surface potentials of aqueous potassium chloride and sodium nitrate (Randles, 1977).

In aqueous ammonium sulfate, however, cations (NH_4^+) reside closer to the surface than anions (SO_4^{2-}). We note here that this principal result of the present simulations is supported by the measured positive surface potential of aqueous tetramethyl ammonium sulfate (Randles, 1957). A qualitative explanation of the positive polarity of the surface layer of ammonium sulfate is based on the fact that due to a large increase in ion-water electrostatic interactions dianions solvate significantly better than ions carrying a single charge. This is in accord with the position of the two ions in the Hofmeister series (Cacace et al., 1997), which places sulfate (ammonium) among strongly (weakly) solvated ions.

4. Results of molecular dynamics simulations

This principal result of the simulation is that aqueous ammonium cations and sulfate dianions have different interfacial concentrations. While in the bulk solution, the concentration ratio between the two ionic species, ammonium cations and sulfate dianions, equals to 2:1, we see an enhanced propensity of ammonium for the solution/air interface. This is clearly demonstrated in Fig. 2, which shows the density profiles, i.e., concentrations of individual species along the direction perpendicular to the open surface, from the centre to the interface. The signal from water oxygen defines the spatial extent of the slab with the solution/air interface between 1.3 and 1.7 nm. We see that all sulfate dianions solvate deep in the aqueous bulk with very little signal beyond 1 nm. The behaviour of ammonium cations is very different. Although the majority of the cations resides in the interior, there is an appreciable signal also just below and in the interfacial layer, up to 1.5 nm.

The fact, that ammonium cations reside up to 0.5 nm closer to the solution/air interface than sulfate dianions has direct consequences for the charge transfer during collisions between ice crystals and graupels. Namely, as the neat quasi-liquid interfacial layer of the ice crystal (Furukawa and Nada, 1997; Dash et al., 1995) gets in touch with the thin layer of ammonium sulfate solution covering the graupel, ammonium cations are preferentially transferred along the concentration gradient. This leads to positive charging of the rising ice crystals and negative charging of the falling graupels, in accord with the polarity evolution in standard thunderclouds, with the main positive charge pocket being situated above the negative charge region.

We have modelled the ice crystal-graupel encounter by putting into a close contact a neat water layer with that of an aqueous ammonium sulfate solution. Fig. 3 shows this area of contact at the beginning of the encounter and after 0.15 ns. It can be seen that during this period one ammonium cation and no sulfate dianion has been transferred across the interface. We have followed the dynamics of the system for one nanosecond. Fig. 4 depicts the cumulative number of ammonium cations transferred from the graupel to the ice crystal during this period. We see, that with certain fluctuations corresponding to back-transfer this number steadily increases, reaching roughly three at 1 ns. The more deeply solvated sulfate dianions respond more slowly - as a result we have not recorded a single negative charge transfer during the nanosecond simulation. Thus, the present results support the notion that upon close encounter between the neat quasi-liquid layer at the surface of the ice crystal with the ammonium sulfate solution covering the graupel, ammonium cations are preferentially moved from the latter to the former particle.

Alternatively, we have also simulated a genuine collision of two finite size particles, a model graupel with a model ice crystal. For the sake of computational feasibility we had to scale down the particle sizes from micrometer to nanometer range. This scaling can be justified by the results of a recent molecular dynamics

study of binary collisions of aqueous nanodroplets, which showed that the simulations correlate well with experiments for droplets in the micrometer size range (Svanberg et al., 1998). The collision velocity was chosen so that the impact energy per unit collision area was the same as in a real atmospheric ice crystal-graupel collision. For atmospheric collision velocities of several meters per second this leads to relative velocities in our simulations of the order of several hundreds m/s.

A factor that has a crucial effect on the outcome of the simulated ice crystal-graupel collisions is the impact parameter, which defines the eccentricity of the collision. For the above collision velocities we have found out that collisions with a small impact parameter (head-on collisions) lead to sticking of the ice crystal to the graupel followed by rapid water evaporation. Upon increasing the impact parameter we have found a region of grazing collisions characterized by transfer of water molecules and ions from the graupel to the ice crystal. We have performed tens of such collision simulations for varying initial geometries of the two nanoparticles and slightly different impact parameters. We have always observed transfer of several to several tens of water molecules, 1-8 ammonium cations, and 0-3 sulfate dianions from the graupel to the ice crystal. In all cases, the number of transferred ammonium cations was larger than twice the number of sulfate dianions. Consequently, these collisions led to positive charging of the ice crystal (and negative charging of the graupel) by one or, in some cases, by several elementary charges. Four snapshots from such a typical collision are depicted in Fig. 5. We see that during the grazing collision part of the graupel, containing tens of water molecules, 5 ammonium, and 2 sulfate ions, is transferred to the ice crystal, which leads to a net charge transfer of a single positive elementary charge.

Under certain atmospheric conditions (e.g., biomass burning or forest fires) a large amount of aerosols containing other soluble ions, such as potassium cations and chloride and nitrate anions (Andreae et al., 1998; Lacaux et al., 1992) is released into

the atmosphere. We modelled this situation at a molecular level by simulating liquid slabs of a 1.2 M solutions of potassium chloride and potassium nitrate. The resulting density profiles for KCl are shown in Fig. 6, the results for KNO_3 being very similar. We conclude that for both aqueous KCl and KNO_3, the polarity of the interfacial layer is opposite to that of aqueous ammonium sulfate (see Fig. 2). As a matter of fact, KCl and KNO_3 behave similarly as the majority of inorganic salts (with the exception of salts containing polyvalent anions such as sulfate) creating an interfacial layer of negative polarity, i.e., with anions penetrating significantly closer to the solution/air interface than cations (Jungwirth and Tobias, 2002). Thus, the present simulations indicate that replacing the sulfate dianion with monovalent anions such as chloride or nitrate leads to an opposite polarity of charging during graupel-ice crystal collisions, due to a polarity reversal at the interface of the salt solution covering the graupel.

5. Extrapolations to atmospheric conditions

The direct contact area during a collision of a "spiky" branch of an ice crystal (~10 micrometer size) and a more round graupel (with size ranging from 100 micrometers to several millimetres) can be conservatively estimated as 1 μm^2. It follows from the present molecular dynamics simulations that during a single collision 1 - 3 elementary charges (1.6-4.8 x 10^{-4} fC) can be transferred per 10 nm^2 of contact area. This is equivalent to a charge transfer of 16-48 fC per collision, which is of the same order of magnitude or larger than values reported from laboratory studies.

The present ionic effects on charge transfer are somewhere between masking and additive to the other charge transfer mechanisms that were observed in laboratory experiments with pure water and ice. The results of present simulations are directly testable by experiments similar to those by Berdeklis and List (2001) performed,

however, with ice particles frozen from water containing inorganic salts of atmospherically relevant composition and concentration.

6. Atmospheric observations

The dominance of SO_4^{2-} as the most common anion in CCN is consistent with the observations that negative lightning prevail in ordinary thunderstorms, in which the main charging occurs at T<-10ºC. However, this negative charging is described also by the previously proposed mechanisms, so that solely this observation cannot lend support to the role of the present ionic mechanism. It is more instructive to observe conditions where charging is reversed to positive in the domain of negative charging for neat ice processes, because this reversal could not be explained until now by any other mechanism. We examine below the relation between the ionic composition of aerosols and the polarity of lightning, exploring whether a greater fraction of non-sulfate anions is related to a greater percentage of positive lightning.

Positive anomalies in the percentage of positive lightning that amounted to triple the climatological norm were observed over the USA in smoke plumes from forest fires in southern Mexico (Lyons et al., 1998). The median peak current was increased by over 20 kA for the positive lightning, but decreased for the negative lightning. The mean flash multiplicity values for negative flashes decreased from 2.8 to 1.0-1.4 (Murray et al., 2000). Chemical analysis of the smoke that reached the USA, which was associated with the enhanced percentage of positive lightning, showed that the fraction of nitrate and organic anion was greater than in the ambient aerosols (Kreidenweis, 2001). A very clear signal was also obtained from cumulimbus clouds fed directly from forest fires (pyrocumulus) in the USA and Canada. Latham (1991) documented that a large prescribed fire in Canada caused a pyrocumulus that had produced exclusively 21 positive cloud to ground flashes, whereas other

thunderclouds in the vicinity that did not ingest the smoke produced tens of “normal” negative flashes. Vonnegut et al. (1995) reviewed several more similar reports, and concluded that the charge generation and separation mechanism in the cloud, rather than that connected to the fire, was responsible for the resulting anomalous behaviour of the lightning. This conclusion was reinforced by Latham (1999).

Conversely, the highly sulfatic urban air pollution at the same general area as discussed in the beginning of the previous paragraph, over Houston, Texas, was observed to have exactly the opposite effect on the lightning (Steiger et al., 2002). A decrease of 12% in the percentage of positive flashes is observed over the city. Higher negative median peak currents were also observed. In non-urban areas, smoke from tropical forest fires has the largest fraction of sulfate anions and hence a reduced potential to induce positive lightning compared to smoke from temperate forests or grasslands (Yamasoe et al., 2000; Turn et al., 1997). The sulfate content of the smoke typically increases as it matures because of deposition and oxidation of SO_2 on the smoke particles (Reid et al., 1998). This might explain why positive lightning does not dominate the thunderstorms that develop in the extensive mature smoke from the Amazon rain forest (Williams, 2003).

An alternative new explanation for the role of aerosols in charge reversal can be related to their impact of suppressing the precipitation in the cloud, leaving greater amount of supercooled cloud water at greater heights and lower temperature (Rosenfeld, 1999; Rosenfeld, 2000), which have already been suggested to lead to positive charging. This might indeed be operative, but it cannot readily explain the enhanced negative charging over the sulfatic air pollution of Houston, versus the positive charging enhancement in smoke from forest fires.

The present ionic mechanism provides us also with a new way to interpret the reports of strong relations between burned areas and frequency of positive lightning at

the Mackenzie River Basin in northwest Canada. The authors of that study (Kochtubjada et al., 2002) suggested that positive lightning strokes were probably responsible for igniting the fires, because positive cloud to ground flashes are typically more energetic and their current persists longer than for negative flashes (Latham and Williams, 2001). Similar situation was reported in Florida. Quoting from the web site of the COMET outreach program (Comet, 2002): "*It is worth noting that negative flashes started approximately 85% of the lightning fires between 25 May and 4 July 1998; however the ratio of fires to flashes was higher for positive flashes across the state (238 flashes were within 800m of 192 fire locations)*". We suggest the possibility that it is the dearth of sulfates in the fresh smoke that contributes to the formation of the positive lightning. It might well be that the positive lightning induced by smoke ignited new fires that emitted even more smoke, spinning thus a positive feedback loop.

Acknowledgment

We are grateful to Paul Crutzen, Clive Saunders, and Daniel Knopf for valuable discussions and to Earle Williams for his valuable comments. Support (to PJ) from the Czech Ministry of Education (Grant LN00A032) and the US National Science Foundation (Grant CHE-0209719) is gratefully acknowledged.

References

1. Aagard, K., Carmack, E. C., 1989. The role of sea-ice and other fresh water in the Arctic circulation. J. Geophys. Res. 94, 14485-14498.

2. Andreae M. O., Andreae, T. W., Annegarn, H., Beer, J., Cachier, H., le Canut, P., Elbert, W., Maenhaut, W., Salma, I., Wienhold, F. G., Zenker, T., 1998. Airborne studies of aerosol emissions from savanna fires in southern Africa: 2. Aerosol chemical composition. J. Geophys. Res. 103, 32119-32128.

3. Baker, B., Baker, M. B., Jayaratne, E. R., Latham, J., Saunders, C.P.R., 1987. The influence of diffusional growth-rates on the charge-transfer accompanying rebounding collisions between ice crystals and soft hailstones. Q. J. R. Meteor. Soc. 113, 1193-1215.

4. Berdeklis, P., List, R., 2001. The ice crystal-graupel collision charging mechanism of thunderstorm electrification. J. Atmos. Sci. 58, 2751-2770.

5. Boudon, S., Wipff, G., 1991. Free energy calculations involving NH_4^+ in water. J. Comp. Chem. 12, 42-51.

6. Cacace, M. G., Landau, E. M., Ramsden, J. J., 1997. The Hofmeister series: salt and solvent effects on interfacial phenomena. *Q. Rev. Biophys. 30*, 241-277.

7. Caldwell, J., Dang, L. X., Kollman, P. A., 1990. Implementation of nonadditive intermolecular potentials by use of molecular dynamics: Development of a water-water potential and water-ion cluster interactions. J. Am. Chem. Soc. 112, 9144-9147.

8. Case, D. A. et al., 1999. Amber 6 (University of California, San Francisco).

9. Clegg, S. L., Brimblecombe, P., Wexler, A. S., 1998. Thermodynamic model of the system H^+-$NH4^+$-SO_4^{2-}-NO_3^--H_2O at tropospheric temperatures. J. Phys. Chem. A 102, 2137-2154.

10. Comet, 2002. Outreach program, sponsored by the National Weather Service: http://www.comet.ucar.edu/outreach/9915814.htm

11. Dang, L. X., 2002. Computational study of ion binding to the liquid interface of water. J. Phys. Chem. B 106, 10338-10394.

12. Dash, J. G., Fu, H., Wettlaufer, J. S., 1995. The premelting of ice and its environmental consequences. Rep. Prog. Phys. 58, 115-167.

13. Dash, J. D., Mason, B. L. , Wettlaufer, J. S., 2001. Theory of charge and mass transfer in ice-ice collisions. J. Geophys. Res. 106, 20395-20402.

14. Frisch, M. J. et al., 1998. Gaussian98 (Gaussian Inc.: Pittsburgh, PA).

15. Furukawa, Y., Nada, H., 1997. Anisotropic surface melting of an ice crystal and its relationship to growth forms. J. Phys. Chem. B 101, 6167-6170.

16. Gross, G. W., Svec, R. K., 1997. Effect of ammonium on anion uptake and dielectric relaxation in laboratory grown ice columns. J. Phys.Chem. B 101, 6282.

17. Jayarante, E. R., Saunders, C. P. R., Hallet, J., 1983. Laboratory studies of the charging of soft hail during ice crystal interactions. Q. J. R. Met. Soc. 109, 609-630.

18. Jungwirth, P., Tobias, D. J., 2002. Chloride anion on aqueous clusters, at the air-water interface, and in liquid water: Solvent effects on Cl^- polarizability. J. Phys. Chem. A 106, 379-383.

19. Jungwirth, P., Tobias, D. J., 2002. Ions at the air/water interface. J. Phys. Chem. B 106, 6361-6373.

20. Jungwirth, P., Curtis, J. E., Tobias, D. J., 2003. Polarizability and aqueous solvation of sulfate dianion. Chem. Phys. Lett. 367, 704-710.

21. Kochtubjada, B., Stewart, R. E., Gyakum, J. R., Flannigan, M. D., 2002. Summer convection and lightning over the Mackenzie River basin and their impacts during 1994 and 1995. Atmos.-Ocean **40**, 199-220.

22. Kreidenweis, S.M., Remer, L.A., Bruintjes, R., Dubovik, O., 2001. Aerosol from biomass burning in Mexico: Hygroscopic smoke optical model. J. Geophys. Res. 106, 4831-4844.

23. Lacaux, J. P., Loembandembi, J., Lefeivre, B., Cros, B., Delmas, R., 1992. Biogenic emissions and biomass burning influences on the chemistry of the fogwater and stratiform precipitation in the African equatorial forest. Atmos. Environment 26, 541-551.

24. Lang, T. J., Rutledge, S. A., 2002. Relationships between convective storm kinematics, precipitation, and lightning. Month. Weather Rev. 130, 2492-2506.

25. Latham, D. J., 1991. Lightning flashes from a prescribed fire influenced cloud. J. Geophys. Res. 96, 17151-17157.

26. Latham, D. J., 1999. Space charge generated by wind tunnel fires. Atmos. Res. 51, 267-278.

27. Latham, D., Williams, E. R., 2001. in: Lightning and forest fires. Forest fires-behavior and ecological effects. (Ed. Johnson, E. A. & Miyanashi, K. Academic Press, New York).

28. Lyons, W. A., Nelson, T. E., Williams, E. R., Cramer, J. A., Turner, T. R., 1998. Enhanced positive cloud-to-ground lightning in thunderstorms ingesting smoke from fires. Science 282**,** 77-80.

29. Mulvaney, R., Wolff, E. W., Oates, K., 1998. Sulphuric acid at grain-boundaries in Antarctic ice. Nature 331, 247-249.

30. Murray, N.D., Orville, R.E., Huffines, G.R., 2000. Effect of pollution from Central American fires on cloud-to-ground lightning in May 1998. Geophys. Res. Lett. 27, 2249-2252.

31. Nelson, J., Baker, M., 2003. Charging of ice-water interfaces: aplications to thunderstorms. Atmos. Chem. Phys. 3, 1-16.

32. Orville, R. E., Huffines, G. R., 2001. Cloud-to-ground lightning in the United States: NLDN results in the first decade, 1989–98. Month. Weather Rev. 129, 1179-1193.

33. Petrenko, V. F., Whitworth, R. W., 1999. Physics of Ice (Oxford University, Oxford).

34. Randles, J. E. B., 1957. Ionic hydration and the surface potential of aqueous electrolytes. Discuss. Faraday Soc. 24, 195-199.

35. Randles, J. E. B., 1977. Structure at the free surface of water and aqueous electrolyte solutions. Phys. Chem. Liq. 7, 107-179.

36. Reid, J. S., Hobbs, P. V., Ferek, R. J., Blake, D. R., Martins, J. V., Dunlap, M. R., Liousse, C. 1998. Physical, chemical, and optical properties of regional hazes dominated by smoke in Brazil. J. Geophys. Res. 103, 32059-32080.

37. Reynolds, S. E., Brook, M., Gourley, M. F., 1957. Thunderstorm charge separation. J. Met. 14, 426-436.

38. Rosenfeld, D., 1999. TRMM observed first direct evidence of smoke from forest fires inhibiting rainfall. Geophys. Res. Lett. 26, 3105-3108.

39. Rosenfeld, D., 2000. Suppression of rain and snow by urban and industrial air pollution. Science 287, 1793-1796.

40. Signorini, G. F., Barrat, J.-L., Klein, M. L., 1990. Structural relaxation and dynamical correlations in a molten state near the liquid-glass transition: A molecular dynamics study. J. Chem. Phys. 92, 1294-1303.

41. Sommer, A. P., Levin, Z., 2001. Charge transfer in convective thunderclouds induced by molecular interface crossing and free energy reduction. Atmos. Res. 58, 129-139.

42. Steiger, S.M., Orville, R.E., Huffines G. R., 2002. Cloud-to-ground lightning characteristics over Houston, Texas: 1989-2000. J. Geophys. Res. 107, 4117-4126.

43. Straatsma, T. P., Berendsen, H. J. C., 1988. Free energy of ionic hydration: Analysis of a thermodynamic integration technique to evaluate free energy differences by molecular dynamics simulations. J. Chem. Phys. 89, 5876-5886.

44. Svanberg, M., Ming, L., Markovic, N., Pettersson, J. B. C., 1998. Collision dynamics of large water clusters. J. Chem. Phys. 108, 5888-5897.

45. Takahashi, T., 1978. Riming electrification as a charge generation mechanism in thunderstorms. J. Atmos. Sci. 35, 1536–1548.

46. Takahasi, T., M. Miyawaki, K., 2002. Reexamination of Riming Electrification in a Wind Tunnel. J. Atmos. Sci. 59, 1018–1025.

47. Thibert, E., Domine, F., 1997. Thermodynamics and kinetics of the solid solution of HCl in ice. J. Phys.Chem. B 101, 3554-3565.

48. Thibert, E., Domine, F., 1997. Thermodynamics and kinetics of the solid solution of HNO_3 in ice. J. Phys.Chem. B 102, 4432.

49. Turn, S. Q., Jenkins, B. M., Chow, J. C., Pritchett, L. C., Capbell, D., Cahill, T., Whalen, S. A., 1997. Elemental characterization of particulate matter emitted from biomass burning: wind tunnel derived source profiles for hebaceous and wood fuels. J. Geophys. Res. 102, 3683-3699.

50. Vonnegut, B., Latham, D. J., Moore, C. B., Hunyady, S. J., 1995. An explanation for anomalous lightning from forest fire clouds. J. Geophys. Res. 100, 5037-5050.

51. Williams, E. R., Zhang, R., Rydock, J., 1991. Mixed phase microphysics and cloud electrification. J. Atmos. Sci. 48, 2195-2203.

52. Williams, E. R., 2003. Personal communications.

53. Wilson, M. A., Pohorille, A., 1991. Interaction of monovalent ions with the water liquid-wapor interface: A molecular dynamics study. J. Chem. Phys. 95**,** 6005-6013.

54. Workman, E. J., Reynolds, S. E., 1950. Electrical phenomena occurring during the freezing of dilute aqueous solutions and their possible relationship to thunderstorm electricity. Phys. Rev. 78, 254-259.

55. Xu, J., Imre, D., McGraw, R., Tang, I., 1998. Ammonium sulfate: Equilibrium and metastability phase diagrams from 40 to -50 ^{o}C. J. Phys. Chem. B 102, 7462-7469.

56. Yamasoe, M. A., Artaxo, P., Miguel, A. H., Allen, A. G., 2000. Chemical composition of aerosol particles from direct emissions of vegetation fires in the Amazon Basin: water-soluble species and trace elements. Atmos. Env. 34, 1641-1653 (2000).

Fig. 1: Regions of negative and positive charging as a function of temperature and the effective cloud water content. This compilation of previous studies is adopted with permission from Ref. 2.

Fig. 2: Density profiles of ammonium and sulfate ions, and water oxygens in an aqueous slab at 275 K. All the profiles are renormalized to equal concentrations. Note the stronger propensity of ammonium cations to the interface compared to sulfate dianions.

Fig. 3: Two snapshots from a simulation demonstrating the transport of NH_4^+ from the graupel to the ice crystal during. a) beginning of the encounter between a neat aqueous layer and an ammonium sulfate solution, and b) transfer of one ammonium cation at t = 0.15 ns. Color coding: oxygen (red), nitrogen (blue), sulfur (yellow), and hydrogen (white). Water hydrogens are not displayed. The translucent region highlights the contact area between the modelled graupel and ice crystal.

Fig. 4: Time evolution of the number of ammonium cations transferred from the graupel to the ice crystal. Note, that all sulfate dianions stayed on the graupel side during the first nanosecond after the encounter.

Fig. 5: Snapshots from a simulations of a grazing collision of a model graupel with an ice nanocrystal leading to a net transfer of one positive elementary charge to the ice crystal. a) Initial geometry (t = 0 ps), b) onset of the grazing collision (t = 10 ps), c) transfer of particles to the ice crystal (t = 15 ps), and d) a zoomed view of the ice crystal with scavenged numerous water molecules, 5 ammonium cations, and 2 sulfate dianions after the collision (t = 30 ps). For better recognition, water oxygens of the ice crystal are displayed in green.

Fig. 6: Density profiles of salt ions and water oxygens in an aqueous slab of a 1.2 M KCl solution. All the profiles are renormalized to equal concentrations. Note the stronger propensity of chloride anions to the interface compared to potassium cations.

Fig. 1 (Jungwirth et al.)

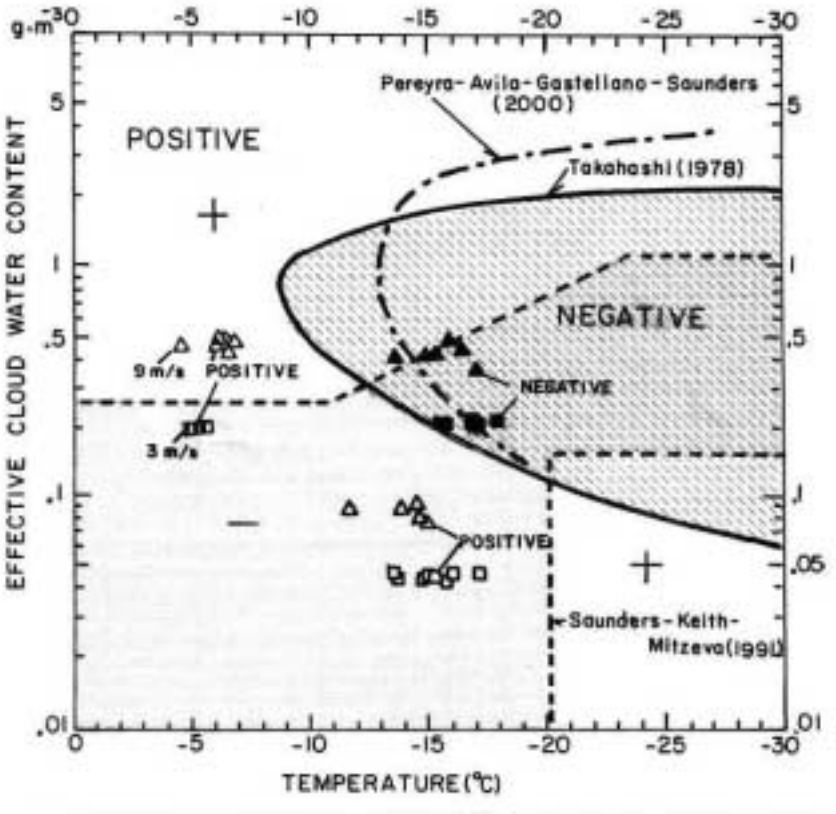

Fig. 2 (Jungwirth et al.)

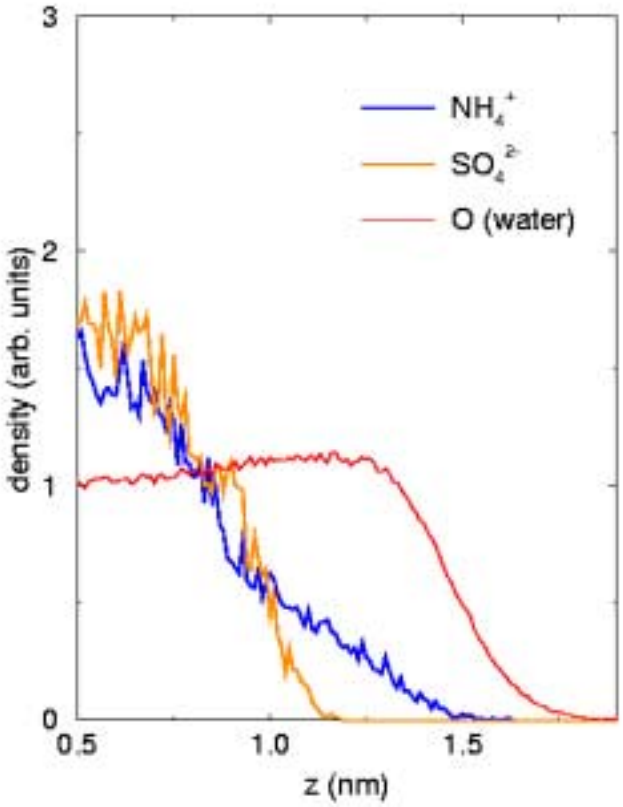

Fig. 3 (Jungwirth et al.)

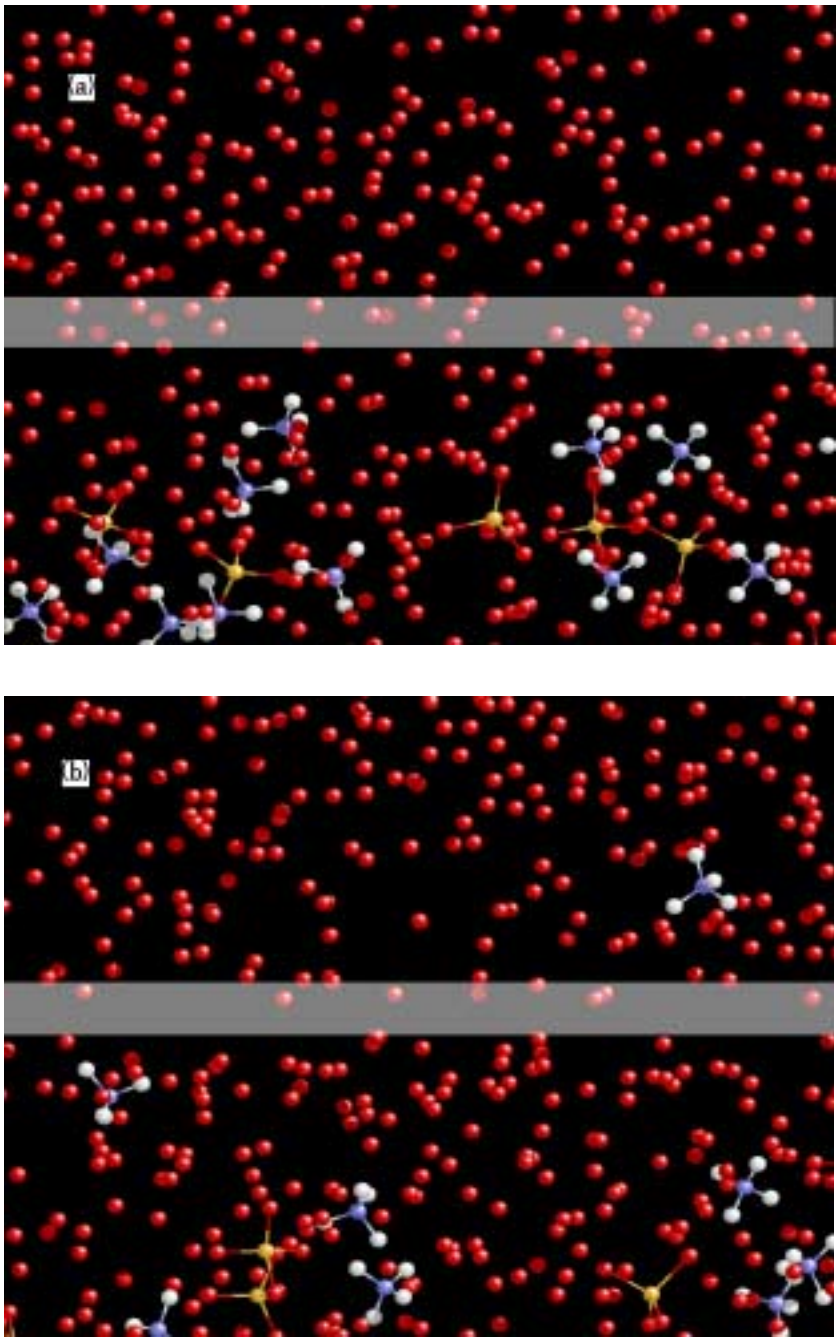

Fig. 4 (Jungwirth et al.)

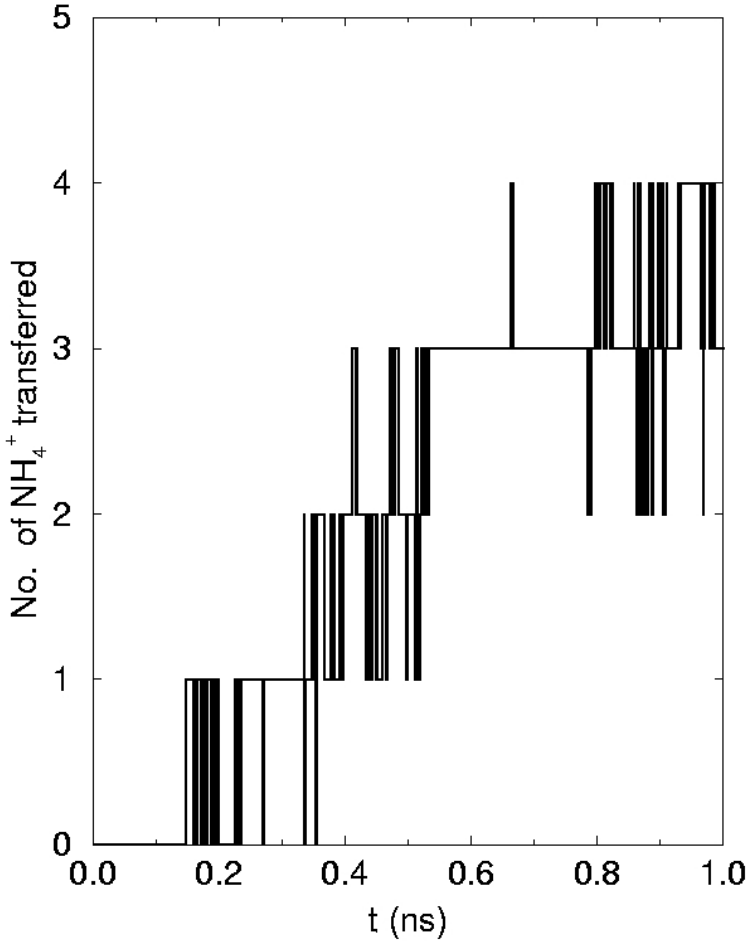

Fig. 5 (Jungwirth et al.)

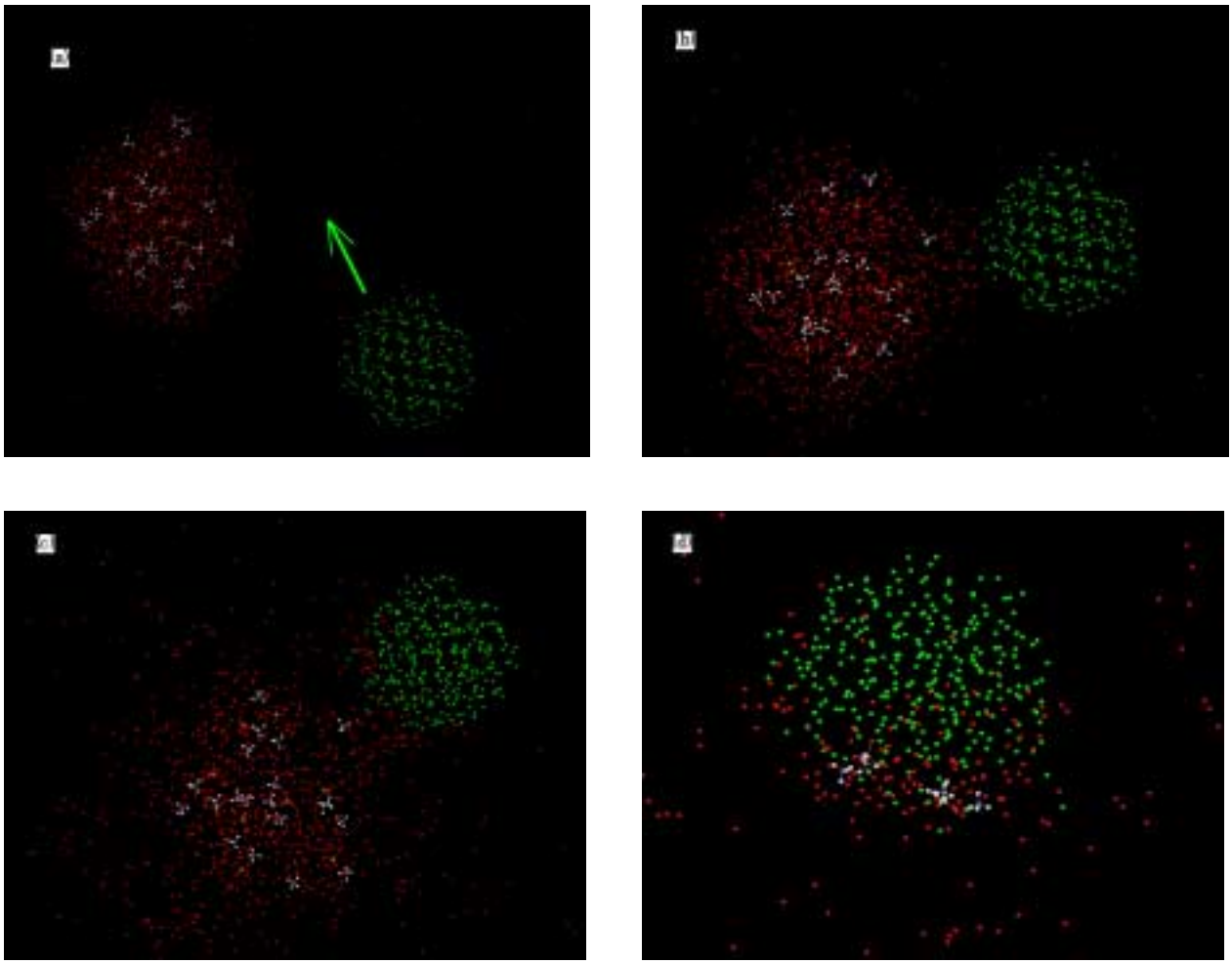

Fig. 6 (Jungwirth et al.)